A Computational Design of siRNA in SARS-CoV-2 Spike Glycoprotein Gene and Its Binding Capability toward mRNA

Arli Aditya Parikesit[1*], Arif Nur Muhammad Ansori[2], and Viol Dhea Kharisma[3]

[1]*Department of Bioinformatics, School of Life Sciences, Indonesia International Institute for Life Sciences, Jakarta 13210, Indonesia*

[2]*Professor Nidom Foundation, Surabaya 60115, Indonesia*

[3]*Computational Virology Research Unit, Division of Molecular Biology and Genetics, Generasi Biologi Indonesia Foundation, Gresik 61171, Indonesia*

* ***Corresponding author:***

email: arli.parikesit@i3l.ac.id

Received: August 14, 2021
Accepted: June 23, 2022

DOI: 10.22146/ijc.68415

Abstract: *COVID-19 pandemic has no immediate ending in sight, and any significant increasing cases were observed worldwide. Currently, there are only two main strategies for developing COVID-19 drugs that predominantly use a proteomics-based approach, which are drug repurposing and herbal medicine strategies. However, a third strategy has existed, called small interfering RNA or siRNA, which is based on the transcriptomics approach. In the case of SARS-CoV-2 infection, it is expected to perform by silencing the viral gene, which brings the surface glycoprotein (S) gene responsible for SARS-CoV-2 viral attachment to the ACE2 receptor on the human host cell. This third approach applies a molecular simulation method comprising data retrieval, multiple sequence alignment, phylogenetic tree depiction, 2D/3D structure prediction, and RNA-RNA molecular docking. The expected results are the prediction of 2D and 3D structures of both siRNA and mRNA silenced S genes along with a complex as the result of a docking method formed by those silenced genes. An Insilco chemical interaction study was performed in testing siRNA and mRNA complex's stability with the confirmation result of a stable complex which is expected to be formed before mRNA reaches the ribosome for the translation process. Thus, siRNA from the S gene could be considered a candidate for the COVID-19 therapeutic agent.*

Keywords: *COVID-19; SARS-CoV-2; siRNA; S gene; molecular docking*

■ INTRODUCTION

COVID-19 is an upper respiratory tract disease caused by the SARS-CoV-2 virus [1-2]. COVID-19 pandemic has contributed to almost 520 million cases and more than 6 million mortalities to date (per 12th of May 2022). However, WHO has yet made any endorsement for anti-SARS-CoV-2 drugs. Any previously supported drugs, such as redeliver and hydroxychloroquine, are paused for further review [3]. In contrast, endorsement of interleukin blockers and dexamethasone as COVID-19 drugs are given only for severe or critical patients. Even though these drugs are not directly stated as antiviral, they ameliorate the overreaction of the immune system post-SARS-CoV-2 infection [4-5]. In this regard, there is room for improvement in designing anti-SARS-CoV-2 therapy.

Furthermore, the SARS-CoV-2 genome is considered larger compared to any other RNA virus, such as influenza and HIV [6]. Hence, it draws a complicated repertoire of protein-protein interactions encompassing various viral activities such as host attachment, infection, and replications [7]. Then, one of the focal points for COVID-19 drug design is by blocking the virulence of its viral particle [8]. SARS-CoV-2 virus' infectivity or virulence is mainly delivered by its spike protein located on the viral surface [9]. It plays an important role in viral penetration to the host cell by facilitating the attachment to ACE2 receptors [10]. Thus, it is logical in the sense of rational drug design that SARS-CoV-2 spike protein should be inhibited to ward off viral infection [11]. However,

although it is considered the primary paradigm for drug design, the proteomics-based approach currently does not confer any significant number of COVID-19 WHO-endorsed drugs [2-4,12]. In fact, until recently, there was no significant breakthrough in COVID-19 drug design studies. Even worse, the pandemic ravaged to the new escalation as the SARS-CoV-2 delta variant appeared (Pango Lineage: B.1.617.2) as the variant of concern (VOC) with much higher infection and hospitalization rate ever worldwide [13-15]. Furthermore, it is also known that the SARS-CoV-2 delta variant has 1000 times more viral loads than the original SARS-CoV-2 strain [16]. In this regard, the transcriptomics-based pipeline could be considered a breakthrough [17]. The transcriptomics-based drug works by leveraging RNA as a therapeutic agent [18]. Mainly, siRNA was deployed for deterring other upper respiratory tract viral infections, such as influenza and MERS, and SARS, as proven in the wet laboratory setting [19-23]. The very principle of siRNA deployment is so-called 'preemptive striking', which blocks the viral genes before upregulating the protein expression [24].

Meanwhile, structural bioinformatics, as the application of computational chemistry in the field of molecular biology, has played a pivotal role in the pipeline development for siRNA studies [25-28]. The basics of this approach are the chemical thermodynamics and kinetics theory working under the classical mechanic paradigm [29-32]. The occurring spontaneous reaction is the foundation of molecular docking and dynamics simulations, which become the pillars of drug design [33-35]. Molecular simulation methods which are commonly deployed in proteomics research, have been proven to be successfully applied for any RNA-RNA and/or RNA-Protein simulations with some adjustments [36-37]. Finally, RNA-based molecular simulation is applicable as well for the purpose of designing the COVID-19 drug. The objective of this research was to examine the chemical interaction of siRNA in silencing SARS-CoV-2 S gene mRNA. Lastly, this research would induce a siRNA design, the docking analysis of the siRNA-mRNA complex, and it would be concluded with the result of chemical interaction analysis.

■ EXPERIMENTAL SECTION

Computer Hardware

The research was carried out with a Macbook Pro Retina® computer with 8 GB RAM, Intel® Core™ i5, Intel graphics processor 1.5 GB VRAM, and 256 GB SSD. The deployed software was based on MacOSX 10.4.6 Mojave operating system.

Techniques

The procedure was inspired by the previously developed pipeline for RNA-RNA molecular simulation [38-39]. Specific parameters were added, as mentioned in the subsections below, if necessary. The procedure of subsections below should be followed consecutively for the consistency of the whole pipeline.

Data Retrieval

The NCBI virus website was accessed from https://www.ncbi.nlm.nih.gov/labs/virus/ [40]. Then, a Tabular view was selected, and the nucleotide tab was clicked. The following search criteria for the data annotation were applied: Virus (SARS-CoV-2, taxid: 2697049); Sequence length (100–1000 bp); Nucleotide completeness (partial); Proteins (Surface glycoprotein); Geographic region (Africa, Asia, and South America); Collection date (Nov 16, 2020, to May 18, 2021); Host (Homo sapiens, TaxId: 9605); and Sequence type (GenBank). Other parameters are left at default values.

MSA and Phylogenetic Tree

The default MSA (multiple sequence alignment) and phylogenetic tree of NCBI virus applets were deployed. The NCBI virus MSA method was built on the MUSCLE algorithm and previously deployed parameters [39]. ClustalX was employed for NCBI virus downloaded data for MSA annotation. The utilized parameters were Gap Opening: 15; Gap Extension 6.66; Delay Divergent Sequences (%): 30; DNA Transition Weight: 0.5; Use Negative Matrix: Off; Protein Weight Matrix: Gonnet series; and DNA Weight Matrix: IUB. The MSA conserved region was extracted with the default text editor. The parameters used for phylogenetic tree were: Bootstrap NJ tree annotation with Random number

generator seed 111 and number of bootstrap trials 1000.Ph format. The data was then saved as phylip tree format.

RNAxs Application of siRNA Design for Repressing the S Gene mRNA

RNAxs software was accessed through this link: http://rna.tbi.univie.ac.at/cgi-bin/RNAxs/RNAxs.cgi [41]. The conserved region of the MSA section was applied in this pipeline. The utilized parameters were set as follows: 8nt Accessibility Threshold: 0.01157; 16nt Accessibility Threshold: 0.001002; Self Folding Energy: 0.9022; Sequence Asymmetry: 0.5; Energy Asymmetry: 0.4655; Free End: 0.625; Custom Sequence Rules: NNNNNNNNNNNNNNNNNNN; and the maximal number of siRNAs: 3.

Locating siRNA Target's Conserved Region in MSA Results

The .aln file of the MSA result was forwarded to Jalview 2.11 to determine the siRNA target [42].

RNAalifold for Conserved Structure of S Gene's mRNA

RNAalifold software was accessed through the following link: http://rna.tbi.univie.ac.at/cgi-bin/RNAWebSuite/RNAalifold.cgi [43]. The conserved region of the MSA section was applied in this pipeline. The utilized parameters were as follows: RNAalifold version: new RNAalifold with RIBOSUM scoring; Fold algorithms and basic options: minimum free energy (MFE) and partition function; and avoiding any isolated base pairs.

RNAfold for both siRNA and mRNA's 2D Structures

RNAfold software was accessed from this link: http://rna.tbi.univie.ac.at/cgi-bin/RNAWebSuite/RNAfold.cgi [44]. The conserved region of the MSA section was applied in this pipeline. The employed parameters were as follows: Fold algorithms and basic options: minimum free energy (MFE) and partition function; and avoiding any isolated base pairs.

Barrier Server for Determining siRNA and mRNA 2D Structure Diversity

The barrier Server software was accessed at this link: http://rna.tbi.univie.ac.at/cgi-bin/RNAWebSuite/barriers.cgi [45-46]. The Vienna dot-bracket annotation of 2D data annotation was applied in this pipeline. The utilized parameters were as follow: the maximal number of lowest local minima: 50; considered only minima with a barrier higher than: 0.1; avoiding any isolated base pairs; declining energies on both sides of a helix in any case; RNA parameters with Turner model; and rescaling the energy parameters to given temperature (C): 37.

iFoldRNA Iteration for both siRNA and mRNA's Sequences and 2D Structure

An iFoldRNA software was accessed from this link: https://dokhlab.med.psu.edu/ifoldrna/ [47-48]. The Vienna dot-bracket annotation of 2D data annotation and FASTA format was applied in this pipeline. The employed parameters were as follow: simulation time 20000; Replica 1 Temperature (DMD Units) 0.2; Replica 2 Temperature (DMD Units) 0.225; Replica 3 Temperature (DMD Units) 0.25; Replica 4 Temperature (DMD Units) 0.27; Replica 5 Temperature (DMD Units) 0.3; Replica 6 Temperature (DMD Units) 0.333; Replica 7 Temperature (DMD Units) 0.367; Replica 8 Temperature (DMD Units) 0.4; Replica Exchange Interval (DMD units): 1000; Heat Exchange Coefficient (Berendsen Thermostat, DMD Units): 0.1.

Validation of 3D RNA Structures

Molprobity server in http://molprobity.biochem.duke.edu/index.php was used in validating 3D RNA structures with parametric thresholds [49]. The designated parameters for RNA structure validation were all-atom contacts, nucleic acid geometry, and additional validations.

3D Structures' Energy Protonation and Minimization of mRNA and siRNA using AVOGADRO

AVOGADRO molecular editor software was downloaded from: https://avogadro.cc/ [50-51]. RNA data in PDB format was applied in this pipeline. The employed parameters were as follows: Select the 'add hydrogen' option. The tapping of the 'minimize energy' button was performed using the following parameters: force field: UFF; steps per update: 4; and algorithm: Steepest Descent Algorithm.

RNA-RNA Molecular Docking of siRNA and mRNA using HNADOCK

HNADOCK nucleic acid docking software was accessed here: http://huanglab.phys.hust.edu.cn/hnadock/ [52]. RNA data are optimized PDB format was applied in this pipeline. The utilized parameters were RNA secondary structure prediction method: RNAfold; RNA-RNA interaction prediction method: ab initio; and refining the top 10 complex models: yes (Longer molecular dynamic simulation would be provided).

Chemical Interaction Prediction of siRNA and mRNA Complex with IntaRNA

An IntaRNA software was accessed from the following link: http://rna.informatik.uni-freiburg.de/IntaRNA/Input.jsp [53-55]. The Vienna dot-bracket annotations from 2D data annotation and FASTA format were applied in this pipeline. The employed parameters were a number of interactions per RNA pair: 1; suboptimal interaction overlap: an overlap in query; no lonely base pairs; no GU at helix ends; minimum number of base pairs in seed: 7; and ignoring seeds with GU ends.

Prediction of siRNA-mRNA Complex's 3D Chemical Interactions using PLIP

PLIP software was accessed from this website: https://plip-tool.biotec.tu-dresden.de [56]. siRNA-mRNA complex in PDB file format was applied in this pipeline. The employed parameters for detecting macromolecule-ligand interactions were used by treating nucleic acid as a receptor and detecting interactions for 1 model. However, the detection of interactions between the rest of the macromolecule and chain(s) was also accomplished by treating nucleic acid as a receptor and detecting interactions for 1 model.

Data Analysis and Complex Visualization

The data annotation of the siRNA-mRNA complex was visualized with UCSF chimera software version 1.15 [57]. The visualization was focused on observing the chemical structure's integrity and feasibility.

■ RESULTS AND DISCUSSION

S gene entry in GenBank was dominated by DNA sequences from India, possibly due to the shifting COVID-19 pandemic epicenter at that time. Currently (per June 2021), even though with a declining tendency, India has the highest daily cases in the world [58]. Table 1 clearly presents that the delta variant started to dominate S gene annotations from the South Asia region and this condition was in line with the increased transmission of the variant. It also started to replace alpha variants as well in the recently annotated S gene data.

Table 1. The SARS-CoV-2 S gene nucleotide sequences retrieved from GenBank (https://www.ncbi.nlm.nih.gov/labs/virus/vssi)

No.	Accession	Geo location	SARS-CoV-2 variant (Pango lineage/WHO naming)	Collection date
1	MZ149959	India: Assam	B.1.617.2/Delta	23/04/21
2	MZ149960	India: Assam	B.1.617.2/Delta	25/04/21
3	MZ149961	India: Assam	B.1.617.2/Delta	23/04/21
4	MZ149962	India: Assam	B.1.617.2/Delta	22/04/21
5	MZ149963	India: Assam	B.1.617.2/Delta	23/04/21
6	MZ149964	India: Assam	B.1.617.2/Delta	24/04/21
7	MZ149965	India: Assam	B.1.617.2/Delta	23/04/21
8	MZ149966	India: Assam	B.1.617.2/Delta	23/04/21
9	MZ149967	India: Assam	B.1.617.2/Delta	23/04/21
10	MZ149968	India: Assam	B.1.617.2/Delta	23/04/21
11	MZ149973	India: Assam	B.1.617.2/Delta	23/04/21
12	MZ149974	India: Assam	B.1.617	01/05/21
13	MZ149975	India: Assam	B.1.617	16/04/21

No.	Accession	Geo location	SARS-CoV-2 variant (Pango lineage/WHO naming)	Collection date
14	MZ149976	India: Assam	B.1.617	16/04/21
15	MW897354	Iraq	NA	10/02/21
16	MW897355	Iraq	NA	23/03/21
17	MW897356	Iraq	NA	23/03/21
18	MW835152	Uzbekistan: Tashkent, M. Ulugbek district	NA	10/02/21
19	MW835153	Uzbekistan: Tashkent, M. Ulugbek district	NA	10/02/21
20	MW835154	Uzbekistan: Tashkent, Ynusabad district	NA	10/02/21
21	MW835155	Uzbekistan: Tashkent, Ynusabad district	NA	10/02/21
22	MW839583	Uzbekistan: Tashkent, Yunisabad district	NA	11/02/21
23	MW839584	Uzbekistan: Tashkent, Yunisabad district	NA	11/02/21
24	MW828609	Uzbekistan: Tashkent almazar district	NA	13/03/21
25	MW828610	Uzbekistan: Tashkent almazar district	NA	13/03/21
26	MW828611	Uzbekistan: Tashkent almazar district	NA	13/03/21
27	MW828612	Uzbekistan: Tashkent almazar district	NA	13/03/21
28	MW699627	India: Assam	B.1.1.7/Alpha	18/02/21
29	MW699628	India: Assam	B.1.1.7/Alpha	18/02/21
30	MW699629	India: Assam	B.1.1.7/Alpha	24/02/21
31	MW699630	India: Assam	B.1.1.7/Alpha	18/02/21
32	MW648379	India: Assam	B.1.1.7/Alpha	29/01/21
33	MW648380	India: Assam	B.1.1.7/Alpha	29/01/21
34	MW648381	India: Assam	B.1.1.7/Alpha	10/02/21
35	MW646466	Pakistan	NA	02/12/20
36	MW642506	Pakistan	NA	02/12/20
37	MW644688	Pakistan	NA	02/12/20
38	MW644689	Pakistan	NA	02/12/20
39	MW644690	Pakistan	NA	02/12/20
40	MW617293	Pakistan	NA	25/01/21
41	MW617298	Pakistan	NA	25/01/21
42	MW617306	Pakistan	NA	08/02/21
43	MW617312	Pakistan	NA	26/01/21
44	MW617321	Pakistan	NA	26/01/21
45	MW617324	Pakistan	NA	08/02/21
46	MW617325	Pakistan	NA	08/02/21

NOTE: NA, information is not available in the GenBank database

As exhibited in the table, the phylogenetic trees are categorized into three main clusters. Two clusters are dominated by Indian samples, while the others are dominated by Uzbek and Pakistani samples (Fig. 1(a)). Then, in Fig. 1(b), the radiated tree clearly depicts an S gene sample from Pakistan, which has formed an outlier from the clusters. However, the outlier seemed to be evolutionarily closer to the Indian cluster than the Pakistan one. This phenomenon might happen due to the extensive people exchange between the two countries causing both clusters to be closer.

Consequently, mRNA's conserved sequence has served as a siRNA target. Moreover, Fig. 2 illustrates both mRNA and siRNA sequences in the rightmost area of the box. Moreover, this box also displays siRNA as the best-annotated one in the database. Table 2 shows FASTA-formatted sequences for easier process and further annotation efforts.

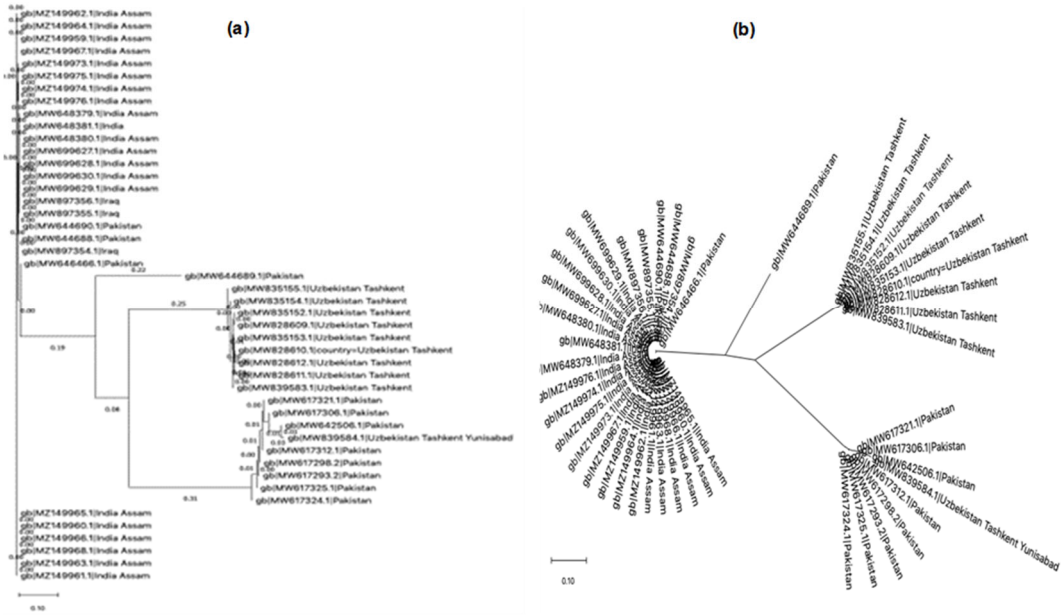

Fig 1. Phylogenetic tree of annotated SARS-CoV-2 S gene from South and Central Asia. (a) Rectangular tree, (b) Radiation tree

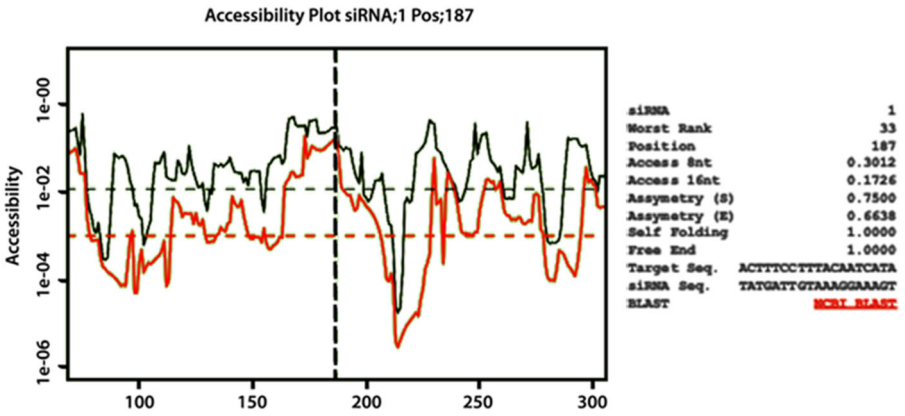

Fig 2. RNAxs output for siRNA of SARS-CoV-2 S gene

Table 2. Annotated ncRNA sequences from RNAxs run of SARS-CoV-2 S gene

Indicator	Value
Rank	33
Position	187
Chosen the best target seq from RNAxs	ACUUUCCUUUACAAUCAUA
Chosen the best siRNA seq from RNAxs	UAUGAUUGUAAAGGAAAGU

Based on the target sequence from RNAxs output above, it is aligned with the consensus sequence of MSA results in Fig. 3. It triggers a significant coverage of consensus regions and exhibits a possibility of siRNA binding in the highlighted region. The consensus region would serve as a foundation for conducting a docking analysis toward the target sequence.

Fig. 4 displays the annotated 2-Dimensional structure of both siRNA's targeted mRNA and its conserved S gene mRNA. Fig. 4(a) is annotated from the

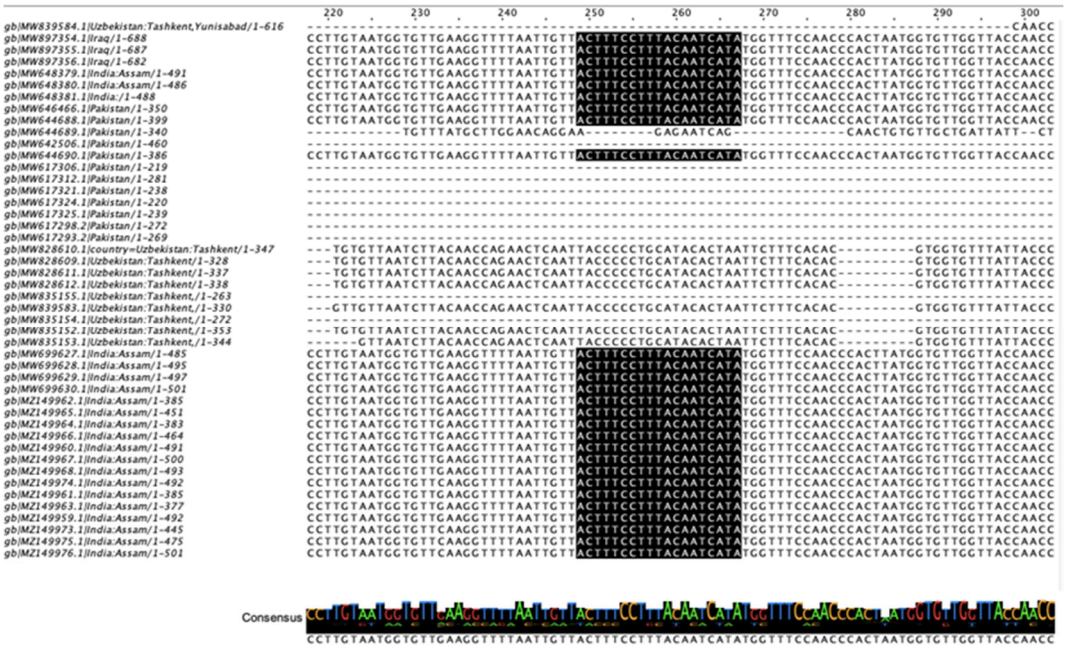

Fig 3. A conserved region of siRNA target in MSA result is highlighted in black. It corresponds to the consensus logo below, and it is the output of JALVIEW 2.11 software

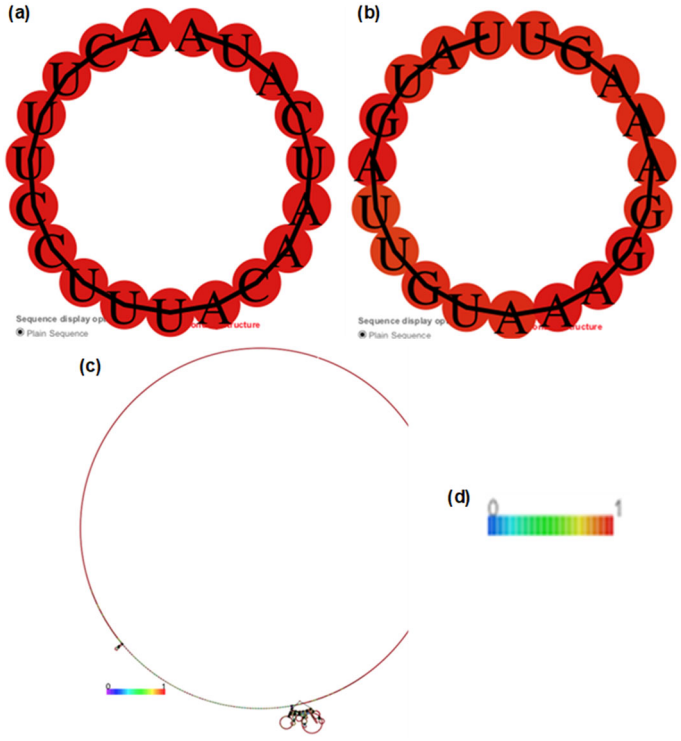

Fig 4. SARS-CoV-2 2D structures prediction (a) S gene mRNA from RNAfold, (b) S gene siRNA from RNAfold, (c) S gene mRNA conserved structure from RNAlifold, (d) A conservation legend, 0 means not conserved, 1 means the most conserved

targeted mRNA gene in Fig. 2. Notably, the minimum free energy prediction of the targeted mRNA is 0.00 kcal/mol; thus, the structure is not considered as spontaneously occurring (Fig. 4(a)). However, siRNA minimum energy is −0.06 kcal/mol indicating a spontaneous structure (Fig. 4(b)). Significantly, the conserved structure minimum energy of S gene mRNA is indicated at −18.62 kcal/mol (Fig. 4(c)). Although it is feasible in a structural manner, the structure has formed an overstretched bulge which is not intuitively feasible in a stereochemical manner. This kind of structure could only exist in a chemical reaction transition state.

Conclusively, it is known from our data that mRNA's structure is singular, not diverse. Thus, the animated structural transition is not feasible to be depicted. The structure of siRNA is more diverse and annotated with three possible conformations, as exhibited in Fig. 5. The very limited number of structural transitions might occur due to the possible steric effects arising from RNA's stereochemical conformation. Moreover, the barrier server only illustrates the transitional structure in a 2D trajectory, thereby limiting the conformational flexibility compared to the 3-dimensional one.

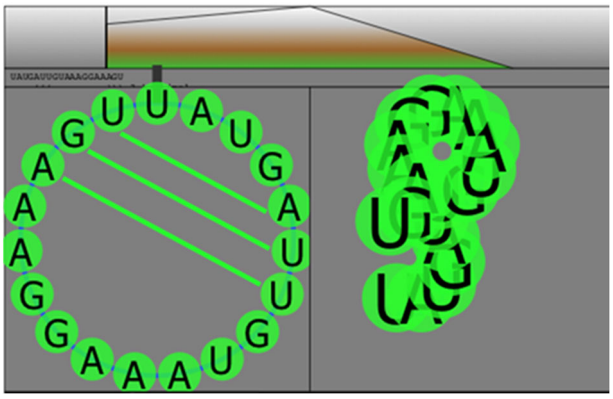

Fig 5. Barrier Server illustration of siRNA 2D conformations

Furthermore, the 3D de novo modeling method has obtained structures of both SARS-CoV-2 S gene conserved mRNA and siRNA (Fig. 6). It displays that both structures differ in their respective conformations. The structure of mRNA clearly expresses a solid loop conformation; therefore, its strand bind to each other (Fig. 6(a)). In contrast, siRNA structure shows a much loose loop conformation because some parts of its strand are not binding to each other (Fig. 6(b)). Regarding 3D structure validation, although they are considered in the warning threshold, both structures produce a near-optimal model that mostly still lies below the quality control threshold of 10% deviation standard from the standard plot (Table 3) [59]. Therefore, it is decided to still proceed with the docking protocol.

Fig. 7 presents the docking results of both mRNA and siRNA structures which have successfully formed a complex. However, the complex visualization using the HNADOCK built-in visualizer is not vivid enough to

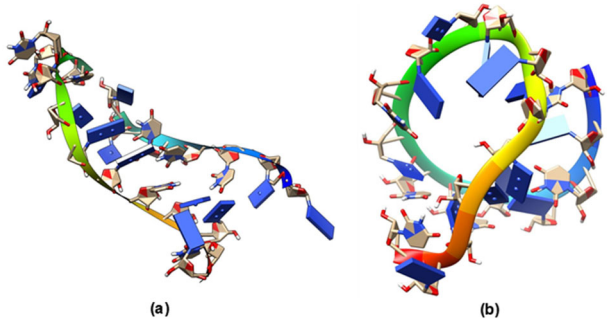

Fig 6. SARS-CoV-2 S gene 3D visualization (a) mRNA, (b) siRNA. Both are illustrated from the result of iFOLDRNA modelling

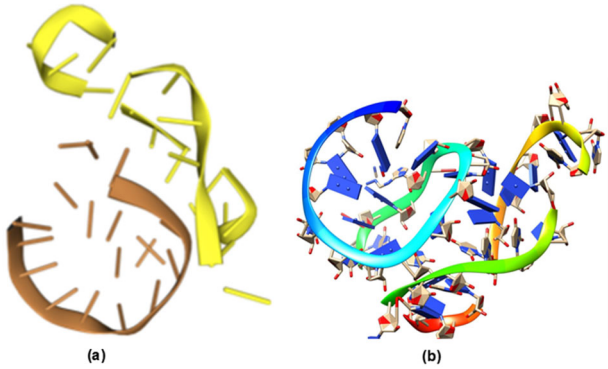

Fig 7. Docking result of SARS-CoV-2 S gene mRNA and siRNA complex (a) Complex visualization using HNADOCK, (b) Complex visualization using UCSF Chimera

Table 3. Molprobity Validation results for RNA 3D Structures. Green is good, yellow is cautious, and red is a warning sign [60]

Indicators	Parameters	siRNA 3D model		mRNA 3D model		Notes
All-atom contacts	Clashscore, all atoms:	206.35		210.72		0th percentile* (N = 1784, all resolutions)
	Clashscore is the number of serious steric overlaps (> 0.4 Å) per 1000 atoms					
Nucleic acid geometry	Probably wrong sugar puckers:	2	10.53%	0	0.00%	Goal: 0
	Bad bonds:	16/460	3.48%	17/434	3.92%	Goal: 0%
	Bad angles:	37/713	5.19%	25/668	3.74%	Goal: < 0.1%
Additional validations	Chiral volume outliers	0/95				
	Waters with clashes	0/0	0.00%			

* The 100th percentile is the best among structures of comparable resolution; the 0th percentile is the worst

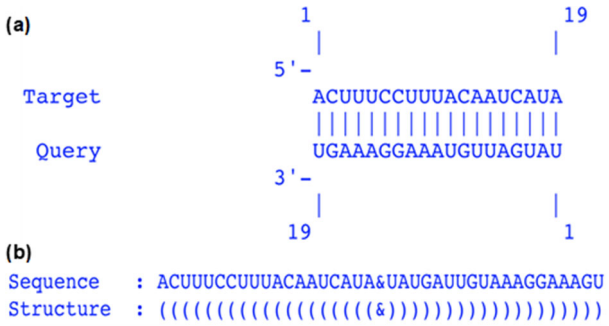

Fig 8. IntaRNA result of SARS-CoV-2 S gene siRNA (Query)-mRNA (Target) complex (a) 2D interactions, (b) Rendition of sequence in FASTA format and structure in Vienna dot-bracket format

observe the conformation (Fig. 7(a)). Thus, the UCSF Chimera visualizer was employed, and a vivid visualization was obtained accordingly (Fig. 7(b)).

The docking visualization has its own limitation in narrating the binding nature because there is no detailed explanation of the involved chemical interactions. Engaging common 2D chemical interactions visualizer such as ligplot+ and leview is not feasible due to their protein-specific scoring function [61-62]. Therefore, Fig. 8expresses the predicted hydrogen bonds between mRNA and siRNA in a 2D fashion. The rendition of IntaRNA software toward the siRNA-mRNA complex could predict the hydrogen bonding of the pairs. However, the notable absence is other types of interactions, such as Van der Waals and hydrophobic ones.

As IntaRNA could only provide a general repertoire of siRNA-mRNA chemical interactions, another software was employed to provide a fine-grained resolution of the bindings. PLIP, a package that is normally utilized for protein-ligand interactions, was applied for this matter. Therefore, as seen in Fig. 9, a higher resolution image of the complex's 3D chemical interactions is exposed accordingly. In the interface of siRNA-mRNA interaction, as seen in Fig. 9, a more specific interaction between Adenosine Triphosphate (ATP) and magnesium ion (Mg^{2+}) appears. In the blue box of Fig. 9, it portrays nine hydrogen bonds and π stacking interactions exposing the resonance between two phenyl groups also exist. These interactions, namely hydrogen bond, metal interaction, and π stacking, are the underlying path for siRNA-mRNA complex integrity.

■ CONCLUSION

It is concluded that based on the current S gene data annotation in the GenBank, the delta variant of SARS-CoV-2 has already gained ground throughout the South Asia region. As this variant has already become a dominant feature worldwide, it would serve as a useful blueprint for drug design. Then, this siRNA for SARS-CoV-2 S gene mRNA was designed from the conserved region annotated with significant numbers of delta variant sequences. Both siRNA and mRNA prediction

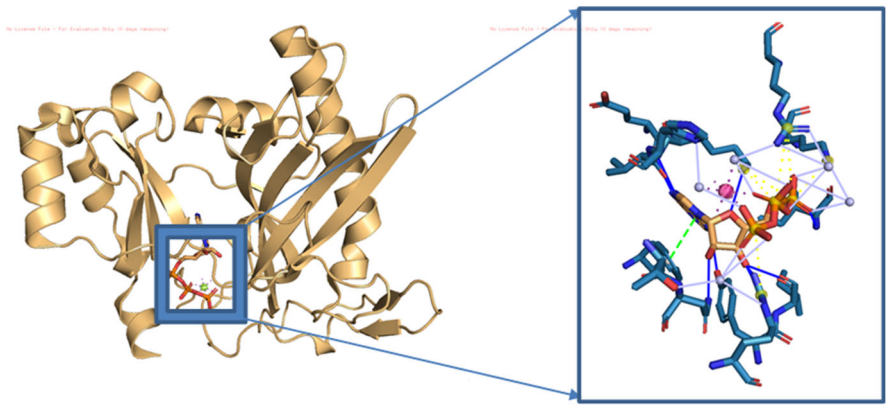

Fig 9. Illustrations of siRNA-mRNA complex with intermolecular siRNA-mRNA interaction, the blue box portray ATP-Mg^{2+} interaction along with the enlarged ATP-Mg^{2+} interactions inside the square. The green ball represents magnesium ions. The red ball represents magnesium ion, while the dashed line represents π-stack, and the straight connecting lines are hydrogen bonding

mechanisms have provided models that could be tested in docking and chemical interaction studies. The chemical interaction studies also produced a high possibility of solid siRNA-mRNA complex integrity. Finally, siRNA design should be elicited in the wet laboratory setting for further validation.

■ ACKNOWLEDGMENTS

The authors would like to thank the Institute of Research and Community Empowerment (LPPM) of Indonesia International Institute for Life Sciences (i3L) for supporting this study. The authors would like to express their gratitude to the Direktorat Sumber Daya, Dirjen DIKTI Kemendikbud-Ristek dan LLDIKTI3 for providing Hibah Penelitian Dasar berbasis Kompetensi 2022 with Ref. No. 0054/E5/AK.04/2022. The authors also gratefully acknowledge the authors, the originating and submitting laboratories for their sequences and metadata shared through NCBI GenBank. Thanks also go to Gilang Valentino from Brandcomm division of i3L for improving the resolution and quality of the manuscript Figures.

■ AUTHOR CONTRIBUTIONS

AAP conducted and supervised the experiment. AAP, ANMA, and VDK wrote and revised the manuscript. All authors agreed to the final version of this manuscript.

■ REFERENCES

[1] Ansori, A.N.M., Kharisma, V.D., Muttaqin, S.S., Antonius, Y., and Parikesit, A.A., 2020, Genetic variant of SARS-CoV-2 isolates in Indonesia: Spike glycoprotein gene, *J. Pure Appl. Microbiol.*, 14, 971–978.

[2] Turista, D.D.R., Islamy, A., Kharisma, V.D., and Ansori, A.N.M., 2020, Distribution of COVID-19 and phylogenetic tree construction of SARS-CoV-2 in Indonesia, *J. Pure Appl. Microbiol.*, 14, 1035–1042.

[3] Agarwal, A., Rochwerg, B., Lamontagne, F., Siemieniuk, R.A.C., Agoritsas, T., Askie, L., Lytvyn, L., Leo, Y.S., Macdonald, H., Zeng, L., Amin, W., Barragan, F.A.J., Bausch, F.J., Burhan, E., Calfee, C.S., Cecconi, M., Chanda, D., Dat, V.Q., De Sutter, A., Du, B., Freedman, F., Geduld, H., Gee, P., Gotte, M., Harley, N., Hashimi, M., Hunt, B., Jehan, F., Kabra, S.K., Kanda, S., Kim, Y.J., Kissoon, N., Krishna, S., Kuppalli, K., Kwizera, A., Castro-Rial, M.L., Lisboa, T., Lodha, R., Mahaka, I., Manai, H., Mino, G., Nsutebu, E., Preller, J., Pshenichnaya, N., Qadir, N., Relan, P., Sabzwari, S., Sarin, R., Shankar-Hari, M., Sharland, M., Shen, Y., Ranganathan, S.S., Souza, J.P., Stegemann, M., Swanstrom, R., Ugarte, S., Uyeki, T., Venkatapuram, S., Vuyiseka, D., Wijewickrama, A., Tran, L., Zeraatkar, D., Bartoszko, J.J., Ge, L., Brignardello-Petersen, R., Owen, A., Guyatt, G., Diaz, J., Kawano-Dourado, L., Jacobs, M., and Vandvik, P.O., 2020, A living WHO guideline on drugs for covid-19, *BMJ*, 370, m3379.

[4] Kharisma, V.D., and Ansori, A.N.M., 2020, Construction of epitope-based peptide vaccine against SARS-CoV-2: Immunoinformatics study, *J. Pure Appl. Microbiol.*, 14, 999–1005.

[5] Kharisma, V.D., Agatha, A., Ansori, A.N.M., Widyananda, M.H., Rizky, W.C., Dings, T.G.A., Derkho, M., Lykasova, I., Antonius, Y., Rosadi, I., and Zainul, R., 2022, Herbal combination from *Moringa oleifera* Lam. and *Curcuma longa* L. as SARS-CoV-2 antiviral via dual inhibitor pathway: A viroinformatics approach, *J. Pharm. Pharmacogn. Res.*, 10 (1), 138–146.

[6] Fernandes, J.D., Hinrichs, A.S., Clawson, H., Gonzalez, J.N., Lee, B.T., Nassar, L.R., Raney, B.J., Rosenbloom, K.R., Nerli, S., Rao, A.A., Schmelter, D., Fyfe, A., Maulding, N., Zweig, A.S., Lowe, T.M., Ares, M., Corbet-Detig, R., Kent, W.J., Haussler, D., and Haeussler, M., 2020, The UCSC SARS-CoV-2 genome browser, *Nat. Genet.*, 52 (10), 991–998.

[7] Parikesit, A.A., 2020, Protein domain annotations of the SARS-CoV-2 proteomics as a blue-print for mapping the features for drug and vaccine designs, *J. Mat. Sains*, 25, 26–32.

[8] Dai, W., Zhang, B., Jiang, X.M., Su, H., Li, J., Zhao, Y., Xie, X., Jin, Z., Peng, J., Liu, F., Li, C., Li, Y., Bai, F., Wang, H., Cheng, X., Cen, X., Hu, S., Yang, X., Wang, J., Liu, X., Xiao, G., Jiang, H., Rao, Z., Zhang, L.K., Xu, Y., Yang, H., and Liu, H., 2020, Structure-

based design of antiviral drug candidates targeting the SARS-CoV-2 main protease, *Science*, 368 (6497), 1331–1335.

[9] Mansbach, R.A., Chakraborty, S., Nguyen, K., Montefiori, D.C., Korber, B., and Gnanakaran, S., 2021, The SARS-CoV-2 spike variant D614G favors an open conformational state, *Sci. Adv.*, 7 (16), eabf3671.

[10] Fahmi, M., Kharisma, V.D., Ansori, A.N.M., and Ito, M., 2021, Retrieval and investigation of data on SARS-CoV-2 and COVID-19 using bioinformatics approach, *Adv. Exp. Med. Biol.*, 1318, 839–857.

[11] Ansori, A.N.M., Kharisma, V.D., Fadholly, A., Tacharina, M.R., Antonius, Y., and Parikesit, A.A., 2021, Severe acute respiratory syndrome coronavirus-2 emergence and its treatment with alternative medicines: A review, *Res. J. Pharm. Technol.*, 14 (10), 5551–5557.

[12] Beigel, J.H., Tomashek, K.M., Dodd, L.E., Mehta, A.K., Zingman, B.S., Kalil, A.C., Hohmann, E., Chu, H.Y., Luetkemeyer, A., Kline, S., Lopez de Castilla, D., Finberg, R.W., Dierberg, K., Tapson, V., Hsieh, L., Patterson, T.F., Paredes, R., Sweeney, D.A., Short, W.R., Touloumi, G., Lye, D.C., Ohmagari, N., Oh, M., Ruiz-Palacios, G.M., Benfield, T., Fätkenheuer, G., Kortepeter, M.G., Atmar, R.L., Creech, C.B., Lundgren, J., Babiker, A.G., Pett, S., Neaton, J.D., Burgess, T.H., Bonnett, T., Green, M., Makowski, M., Osinusi, A., Nayak, S., Lane, H.C., and ACTT-1 Study Group Members, 2020, Remdesivir for the treatment of Covid-19 - Final report, *N. Engl. J. Med.*, 383 (19), 1813–1826.

[13] O'Dowd, A., 2021, Covid-19: Cases of delta variant rise by 79%, but rate of growth slows, *BMJ*, 373, n1596.

[14] Torjesen, I., 2021, Covid-19: Delta variant is now UK's most dominant strain and spreading through schools, *BMJ*, 373, n1445.

[15] Kusumawati, R.L., Lubis, I., Kumaheri, M.A., Pradipta, A., Faksri, K., Mutiara, M., Shankar, A.H., and Tania, T., 2022, Clinical epidemiology of pediatric COVID-19 Delta variant cases from North Sumatra, Indonesia, *Front. Pediatr.*, 10, 810404.

[16] Burnett, J.C., and Rossi, J.J., 2012, RNA-based therapeutics: Current progress and future prospects, *Chem. Biol.*, 19 (1), 60–71.

[17] Reardon, S., 2021, How the Delta variant achieves its ultrafast spread, *Nature*, 10.1038/d41586-021-01986-w.

[18] Yu, A.M., Jian, C., Yu, A.H., and Tu, M.J., 2019, RNA therapy: Are we using the right molecules?, *Pharm. Ther.*, 196, 91–104.

[19] Pashkov, E.A., Faizuloev, E.B., Svitich, O.A., Sergeev, O.V., and Zverev, V.V., 2020, The potential of synthetic small interfering RNA-based antiviral drugs for influenza treatment, *Vopr. Virusol.*, 65 (4), 182–190.

[20] Qiu, M., Li, Y., Bloomer, H., and Xu, Q., 2021, Developing biodegradable lipid nanoparticles for intracellular mRNA delivery and genome editing, *Acc. Chem. Res.*, 54 (21), 4001–4011.

[21] Le, T.K., Paris, C., Khan, K.S., Robson, F., Ng, W.L., and Rocchi, P., 2021, Nucleic acid-based technologies targeting coronaviruses, *Trends Biochem. Sci.*, 46 (5), 351–365.

[22] Yu, A.M., Choi, Y.H., and Tu, M.J., 2020, RNA drugs and RNA targets for small molecules: Principles, progress, and challenges, *Pharmacol. Rev.*, 72, 862–898.

[23] Sohrab, S.S., El-Kafrawy, S.A., Mirza, Z., Kamal, M.A., and Azhar, E.I., 2018, Design and delivery of therapeutic siRNAs: Application to MERS-coronavirus, *Curr. Pharm. Des.*, 24 (1), 62–77.

[24] Hua, K., Jin, J., Zhao, J., Song, J., Song, H., Li, D., Maskey, N., Zhao, B., Wu, C., Xu, H., and Fang, L., 2016, miR-135b, upregulated in breast cancer, promotes cell growth and disrupts the cell cycle by regulating LATS2, *Int. J. Oncol.*, 48 (5), 1997–2006.

[25] Cruz, J.A., Blanchet, M.F., Boniecki, M., Bujnicki, J.M., Chen, S.J., Cao, S., Das, R., Ding, F., Dokholyan, N.V., Flores, S.C., Huang, L., Lavender, C.A., Lisi, V., Major, F., Mikolajczak, K., Patel, D.J., Philips, A., Puton, T., Santalucia, J., Sijenyi, F., Hermann, T., Rother, K., Rother, M., Serganov, A., Skorupski, M., Soltysinski, T., Sripakdeevong, P., Tuszynska, I., Weeks, K.M., Waldsich, C., Wildauer, M., Leontis, N.B., and Westhof, E., 2012, RNA-Puzzles: A CASP-like evaluation of RNA

three-dimensional structure prediction, *RNA*, 18 (4), 610–625.

[26] Hufsky, F., Beerenwinkel, N., Meyer, I.M., Roux, S., Cook, G.M., Kinsella, C.M., Lamkiewicz, K., Marquet, M., Nieuwenhuijse, D.F., Olendraite, I., Paraskevopoulou, S., Young, F., Dijkman, R., Ibrahim, B., Kelly, J., Le Mercier, P., Marz, M., Ramette, A., and Thiel, V., 2020, The international virus bioinformatics meeting 2020, *Viruses*, 12 (12), 1398.

[27] Marz, M., Beerenwinkel, N., Drosten, C., Fricke, M., Frishman, D., Hofacker, I.L., Hoffmann, D., Middendorf, M., Rattei, T., Stadler, P.F., and Töpfer, A., 2014, Challenges in RNA virus bioinformatics, *Bioinformatics*, 30 (13), 1793–1799.

[28] Li, B., Cao, Y., Westhof, E., and Miao, Z., 2020, Advances in RNA 3D structure modeling using experimental data, *Front. Genet.*, 11, 574485.

[29] Kang, Y., and Fortmann, C.M., 2013, An alternative approach to protein folding, *BioMed Res. Int.*, 2013, 583045.

[30] Wei, G., Xi, W., Nussinov, R., and Ma, B., 2016, Protein ensembles: How does nature harness thermodynamic fluctuations for life? The diverse functional roles of conformational ensembles in the cell, *Chem. Rev.*, 116 (11), 6516–6551.

[31] Smerlak, M., 2021, Quasi-species evolution maximizes genotypic reproductive value (not fitness or flatness), *J. Theor. Biol.*, 522, 110699.

[32] Li, C.Y., de Veer, S.J., Law, R.H.P., Whisstock, J.C., Craik, D.J., and Swedberg, J.E., 2019, Characterising the subsite specificity of urokinase-type plasminogen activator and tissue-type plasminogen activator using a sequence-defined peptide aldehyde library, *ChemBioChem*, 20 (1), 46–50.

[33] Seidel, T., Schuetz, D.A., Garon, A., and Langer, T., 2019, The pharmacophore concept and its applications in computer-aided drug design, *Prog. Chem. Org. Nat. Prod.*, 110, 99–141.

[34] Buglak, A.A., Samokhvalov, A.V., Zherdev, A.V., and Dzantiev, B.B., 2020, Methods and applications of in silico aptamer design and modeling, *Int. J. Mol. Sci.*, 21 (22), 8420.

[35] Wang, J., 2020, Fast identification of possible drug treatment of coronavirus disease-19 (COVID-19) through computational drug repurposing study, *J. Chem. Inf. Model.*, 60 (6), 3277–3286.

[36] Parikesit, A.A., and Ramanto, K.N., 2019, The binding prediction model of the iron-responsive element binding protein and iron-responsive elements, *Bioinf. Biomed. Res. J.*, 2 (1), 12–20.

[37] Ivan, J., Nurdiansyah, R., and Parikesit, A.A., 2020, Computational modeling of AGO-mediated molecular inhibition of ARF6 by miR-145, *Indones. J. Biotechnol.*, 25 (2), 102–108.

[38] Valeska, M.D., and Parikesit, A.A., 2020, Structural bioinformatics approach for the molecular models of miR-135b and its silencer as triple negative breast cancer (TNBC) biomarkers, *Horiz. Cancer Res.*, 77, 232–245.

[39] Parikesit, A.A., and Nurdiansyah, R., 2020, The predicted structure for the anti-sense siRNA of the RNA polymerase enzyme (RdRp) gene of the SARS-CoV-2, *Berita Biologi*, 19 (1), 97–108.

[40] Brister, J.R., Ako-Adjei, D., Bao, Y., and Blinkova, O., 2015, NCBI viral genomes resource, *Nucleic Acids Res.*, 43 (D1), D571–D577.

[41] Giulietti, M., Righetti, A., Cianfruglia, L., Šabanović, B., Armeni, T., Principato, G., and Piva, F., 2018, To accelerate the Zika beat: Candidate design for RNA interference-based therapy, *Virus Res.*, 255, 133–140.

[42] Procter, J.B., Carstairs, G.M., Soares, B., Mourão, K., Ofoegbu, T.C., Barton, D., Lui, L., Menard, A., Sherstnev, N., Roldan-Martinez, D., Duce, S., Martin, D.M.A., and Barton, G.J., 2021, Alignment of biological sequences with Jalview, *Methods Mol. Biol.*, 2231, 203–224.

[43] Velandia-Huerto, C.A., Yazbeck, A.M., Schor, J., and Stadler, P.F., 2022, Evolution and phylogeny of microRNAs — Protocols, pitfalls, and problems, *Methods Mol. Biol.*, 2257, 211–233.

[44] Ender, A., Stadler, P.F., Mörl, M., and Findeiß, S., 2022, RNA design principles for riboswitches that regulate RNase P-mediated tRNA processing, *Methods Mol. Biol.*, 2518, 179–202.

[45] Günzel, C., Kühnl, F., Arnold, K., Findeiß, S., Weinberg, C.E., Stadler, P.F., and Mörl, M., 2021, Beyond plug and pray: Context sensitivity and in silico design of artificial neomycin riboswitches, *RNA Biol.*, 18 (4), 457–467.

[46] Stadler, P.F., 2021, Alignments of biomolecular contact maps, *Interface Focus*, 11 (4), 20200066.

[47] Yuan, L., Guo, Z.H., Cao, W.J., Luo, Y., and Shi, Y.Z., 2021, An Integrated Tool for RNA 3D Structure Prediction and Analysis, *2021 33rd Chinese Control and Decision Conference (CCDC)*, 4293–4297.

[48] Krokhotin, A., Houlihan, K., and Dokholyan, N.V., 2015, iFoldRNA v2: Folding RNA with constraints, *Bioinformatics*, 31 (17), 2891–2893.

[49] Williams, C.J., Headd, J.J., Moriarty, N.W., Prisant, M.G., Videau, L.L., Deis, L.N., Verma, V., Keedy, D.A., Hintze, B.J., Chen, V.B., Jain, S., Lewis, S.M., Arendall, W.B., Snoeyink, J., Adams, P.D., Lovell, S.C., Richardson, J.S., and Richardson, D.C., 2018, MolProbity: More and better reference data for improved all-atom structure validation, *Protein Sci.*, 27 (1), 293–315.

[50] Hanwell, M.D., Curtis, D.E., Lonie, D.C., Vandermeersch, T., Zurek, E., and Hutchison, G.R., 2012, Avogadro: An advanced semantic chemical editor, visualization, and analysis platform, *J. Cheminf.*, 4 (1), 17.

[51] Avery, P., Ludowieg, H., Autschbach, J., and Zurek, E., 2017, Extended Hückel calculations on solids using the Avogadro molecular editor and visualizer, *J. Chem. Educ.*, 95 (2), 331–337.

[52] He, J., Wang, J., Tao, H., Xiao, Y., and Huang, S.Y., 2019, HNADOCK: A nucleic acid docking server for modeling RNA/DNA–RNA/DNA 3D complex structures, *Nucleic Acids Res.*, 47 (W1), W35–W42.

[53] Raden, M., Ali, S.M., Alkhnbashi, O.S., Busch, A., Costa, F., Davis, J.A., Eggenhofer, F., Gelhausen, R., Georg, J., Heyne, S., Hiller, M., Kundu, K., Kleinkauf, R., Lott, S.C., Mohamed, M.M., Mattheis, A., Miladi, M., Richter, A.S., Will, S., Wolff, J., Wright, P.R., and Backofen, R., 2018, Freiburg RNA tools: A central online resource for RNA-focused research and teaching, *Nucleic Acids Res.*, 46 (W1), W25–W29.

[54] Raden, M., Müller, T., Mautner, S., Gelhausen, R., and Backofen, R., 2020, The impact of various seed, accessibility and interaction constraints on sRNA target prediction- a systematic assessment, *BMC Bioinf.*, 21 (1), 15.

[55] Mann, M., Wright, P.R., and Backofen, R., 2017, IntaRNA 2.0: Enhanced and customizable prediction of RNA-RNA interactions, *Nucleic Acids Res.*, 45 (W1), W435–W439.

[56] Salentin, S., Schreiber, S., Haupt, V.J., Adasme, M.F., and Schroeder, M., 2015, PLIP: Fully automated protein-ligand interaction profiler, *Nucleic Acids Res.*, 43 (W1), W443–W447.

[57] Butt, S.S., Badshah, Y., Shabbir, M., and Rafiq, M., 2020, Molecular docking using Chimera and Autodock Vina software for nonbioinformaticians, *JMIR Bioinf. Biotechnol.*, 1, e14232.

[58] WHO, 2021, *Novel Coronavirus Disease (Covid-19): Situation Update Report - 50*, World Health Organization, New Delhi, India.

[59] Chen, V.B., Wedell, J.R., Wenger, R.K., Ulrich, E.L., and Markley, J.L., 2015, MolProbity for the masses–of data, *J. Biomol. NMR*, 631 (1), 77–83.

[60] Molprobity, 2021, *Molprobity Legend for Structural Validation*, http://molprobity.biochem.duke.edu/help/validation_options/summary_table_guide.html.

[61] Laskowski, R.A., and Swindells, M.B., 2011, LigPlot+: Multiple ligand-protein interaction diagrams for drug discovery, *J. Chem. Inf. Model.*, 51 (10), 2778–2786.

[62] Caboche, S., 2013, LeView: Automatic and interactive generation of 2D diagrams for biomacromolecule/ligand interactions, *J. Cheminf.*, 5 (1), 40.

[63] Maladan, Y., Krismawati, H., Hutapea, H.M.L., Oktavian, A., Fatimah, R., and Widodo, W., 2019, A new *Mycobacterium leprae* dihydropteroate synthase variant (V39I) from Papua, Indonesia, *Heliyon*, 5 (3), e01279.

[64] Tüzün, B., and Kaya, C., 2018, Investigation of DNA–RNA molecules for the efficiency and activity of corrosion inhibition by DFT and molecular docking, *J. Bio- Tribo-Corros.*, 4 (4), 69.

[65] Yan, Y., and Huang, S.Y., 2020, Modeling protein–protein or protein–DNA/RNA complexes using the HDOCK webserver, *Methods Mol. Biol.*, 2165, 217–229.

[66] Parikesit, A.A., 2021, "Introductory Chapter: The Emerging Corner of the Omics Studies for Rational Drug Design" in *Drug Design - Novel Advances in the Omics Field and Applications*, IntechOpen, Rijeka, 4.

[67] Parikesit, A.A., 2018, "Introductory Chapter: The Contribution of Bioinformatics as Blueprint Lead for Drug Design" in *Molecular Insight of Drug Design*, IntechOpen, Rijeka, 7.

[68] Ivan, J., Agustriawan, D., Parikesit, A.A., and Nurdiansyah, R., 2021, MiRNA-regulated HspB8 as potent biomarkers in low-grade gliomas, *Res. J. Biotechnol.*, 16 (1), 17–25.

[69] Agustriawan, D., Parikesit, A.A., Nurdiansyah, R., Ivan, J., and Ramanto, K.N., 2021, Correlation and transcriptomic analysis revealing potential microRNA-gene interactions associated with breast cancer formation, *Res. J. Biotechnol.*, 16 (2), 16–23.

[70] Medeiros, I.G., Khayat, A.S., Stransky, B., Santos, S., Assumpção, P., and de Souza, J.E.S., 2021, A small interfering RNA (siRNA) database for SARS-CoV-2, *Sci. Rep.*, 11 (1), 8849.

[71] Donia, A., and Bokhari, H., 2021, RNA interference as a promising treatment against SARS-CoV-2, *Int. Microbiol.*, 24 (1), 123–124.

[72] Idris, A., Davis, A., Supramaniam, A., Acharya, D., Kelly, G., Tayyar, Y., West, N., Zhang, P., McMillan, C.L.D., Soemardy, C., Ray, R., O'Meally, D., Scott, T.A., McMillan, N.A.J., and Morris, K.V., 2021, A SARS-CoV-2 targeted siRNA-nanoparticle therapy for COVID-19, *Mol. Ther.*, 29 (7), 2219–2226.

[73] Khaitov, M., Nikonova, A., Shilovskiy, I., Kozhikhova, K., Kofiadi, I., Vishnyakova, L., Nikolskii, A., Gattinger, P., Kovchina, V., Barvinskaia, E., Yumashev, K., Smirnov, V., Maerle, A., Kozlov, I., Shatilov, A., Timofeeva, A., Andreev, S., Koloskova, O., Kuznetsova, N., Vasina, D., Nikiforova, M., Rybalkin, S., Sergeev, I., Trofimov, D., Martynov, A., Berzin, I., Gushchin, V., Kovalchuk, A., Borisevich, S., Valenta, R., Khaitov, R., and Skvortsova, V., 2021, Silencing of SARS-CoV-2 with modified siRNA-peptide dendrimer formulation, *Allergy*, 76 (9), 2840–2854.

[74] Tenda, E.D., Asaf, M.M., Pradipta, A., Kumaheri, M.A., and Susanto, A.P., 2021, The COVID-19 surge in Indonesia: What we learned and what to expect, *Breathe*, 17, 210146.

[75] Dyer, O., 2021, Covid-19: Indonesia becomes Asia's new pandemic epicentre as delta variant spreads, *BMJ*, 374, n1815.

[76] Kupferschmidt, K., and Wadman, M., 2021, Delta variant triggers new phase in the pandemic, *Science*, 372 (6549), 1375–1376.